VOL. 12, NO. 24, DECEMBER 2017 ISSN 1819-6608
ARPN Journal of Engineering and Applied Sciences

www.arpnjournals.com

DESIGN OF SHUNT ACTIVE FILTER USING ITERATIVE METHOD TO MITIGATE THE HARMONICS AND REACTIVE POWER

R. Sriranjani and S. Jayalalitha
Department of Electrical and Electronics Engineering, Sastra University, Thanjavur, Tamil Nadu, India
E-Mail: mathusri@eee.sastra.edu

ABSTRACT

The performance of the Shunt active filter depends upon the design of the filter components and control algorithm used to generate the reference current for the switching controller for the power device of the filter. The Shunt Active filter components are the filter inductance, dc link capacitance and power rating of the switching device. The filter inductance depends upon the switching frequency and dc link capacitance. The design of filter requires the basic electrical parameters obtained from Hilbert and wavelet transform. An Iterative method is adopted to design the filter components to minimize the ripple content of filter current and dc bus voltage of the Shunt active filter. The designed filter is switched by the average dq frame control algorithm generates the fundamental reference current and hysteresis controller compares reference current from the supply current. The average dq frame based Shunt active filter is compared with synchronous reference frame controller by developing the system configuration in MATLAB Simulink and the results are verified.

Keywords: shunt active filter, control algorithm, hysteresis controller, MATLAB, Simulink.

1. INTRODUCTION

An increase in solid state device based power load contaminates the power quality and needs a flexible and efficient solution. A conventional solution to improve the power quality is the Shunt LC filters which however has the undesirable characteristics of possible resonances with source and/or load impedances [1-3]. The above mentioned limitations of the passive filter are eliminated by using Active Filters which employ feedback principles. Shunt Active Filter eradicates the harmonic pollution produced by current type nonlinear loads operating from a 3-phase supply [4]. This filter gives an effective solution for the compensation of current harmonics generated by the non linear loads. Further they are also used to contribute fundamental reactive power due to inductive loads and to balance the source currents due to different single phase loads. The effective performance of the Active Filter depends upon five factors namely (1) Active filter configuration (2) Design of filter parameters (3) Closed loop control strategy (4) Technique used for reference signal generation and (5) Modulation schemes. Out of the five factors, this chapter presents the design of the Shunt Active Filter so that the ripple content of filter current and dc link voltage of SAF is minimized and efficiency of the SAF is maximized.

2. DESIGN OF SHUNT ACTIVE FILTER

The design of the 3-phase Shunt Active Filter involves the calculation of power rating of switching devices and size of the passive components (Lf and Cdc). The main circuit of Voltage Source Shunt Active Filter is depicted in Figure-1. The purpose of the DC link capacitor (Cdc) is [5]: (i) to sustain the Vdc with least ripple in steady state (ii) to serve as an energy storage element to provide the reactive/harmonic power of the load and (iii) to provide the active power difference between the load and source during the transient period. The selection of the high value of capacitance and choosing proper value of reference dc bus voltage (Vdc,ref) of the Active filter, serves the above purposes. The size of capacitor depends upon the switching frequency, thus low switching frequency is selected to serve the functions. The supply of real/reactive power by the Shunt Active Filter charges/discharges the capacitor voltage. This introduces ripples in the dc bus voltage and it is minimized by the controller. Thus the dc bus voltage is maintained constant to a reference value (Vdc,ref).

The selection of the reference value should be in such a way that Cdc should perform the above functions. During variable load conditions, dc bus voltage is increased beyond the reference value to serve the power difference between the load and source. For satisfactory performance of SAF, the peak amplitude of reference current is adjusted proportionally to the change in power difference thus the dc bus voltage reaches the reference value.

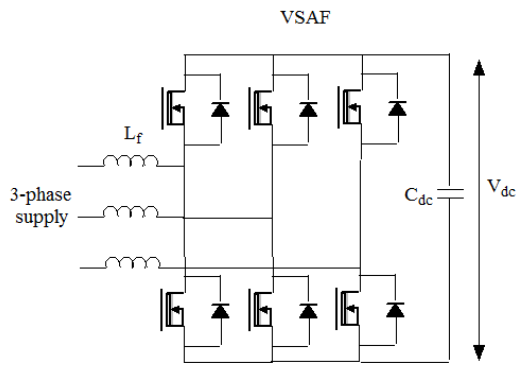

Figure-1. Circuit diagram of 3-phase shunt active filter.

The minimum value of reference voltage should be greater than at-least two times of amplitude of 1- phase supply voltage.

The low switching frequency results in selection of high value of filter inductance which minimizes the ripples in the filter current. In order to select the size of filter inductance, dc link capacitance and the maximum reference value of dc bus voltage, an iterative procedure is followed which minimizes the ripple content of filter current and dc bus voltage. A proper design of passive components improves the performance of filter. The step by step procedure of the design of the filter involves the following calculation of the variables from the known values of three phase instantaneous supply voltage and current.

- Derivation of RMS value of voltage and current, apparent power, fundamental current and phase angle, compensating voltage and current
- Derivation of Total Harmonic Distortion (THD) and maximum kVA rating of VSI
- Initialization of reference DC bus voltage, ripple content of filter current (ΔI_f), DC voltage (ΔV_{dc}) and switching frequency(f_{sw})
- Derivation of the initial values of filter inductance (L_f) and dc bus capacitance (C_{dc})
- Derivation of rate of change of filter current and load current.

3. INITIALIZATION OF FILTER DESIGN PARAMETERS

The design of 3 - phase Shunt Active Filter involves the selection of the filter inductor (L_f), dc link capacitor (C_{dc}) and power rating of the SAF (SSAF). It is based on the initialization of parameters like switching frequency, minimum reference DC bus voltage, ripple content of filter current and DC link voltage.

a) Design of filter inductor (L_f)

The 3-phase filter inductor is introduced in SAF to reduce the ripples of the filter current (compensating current) so the design of the inductor is focused on the compensating current.

It is based on the following criterion [6]

a) Minimizing the high frequency component of compensating currents
b) The maximum di_l/dt of the load should be less than the instantaneous di_f/dt_{max} generated by the SAF

From the above assumptions, ripple current is determined by,

$$\Delta i_f(t) = \frac{1}{2L_f}\int_0^{T_s/2}\left(V_f(t) - V_s(t)\right)dt \tag{1}$$

Where, $V_f(t) = f_{sw}(t)\frac{V_{dc,ref}}{2}$ $f_{sw}(t)$ is the switching frequency that defines the duty cycle of the power devices and Vs(t) is the 1- phase supply voltage. Solving the equation. (1), the filter inductance is given by,

$$L_f \approx \frac{\pi\left(V_{dc,ref} - 2\hat{V}_s\right)}{2\omega_{sw}\Delta I_{f\max}} \tag{2}$$

The filter inductance value is inversely proportional to the switching frequency and ripple content of filter current.

b) Reference DC bus voltage of SAF

Choosing the proper value of $V_{dc,\,ref}$, reduces the ripples of dc bus voltage. The dc bus voltage depends upon the maximum phase voltage. The minimum value of the dc reference voltage is considered from the equation (2), given by [7, 8],

$$V_{dc,\min} > 2\times\hat{V}_s \tag{3}$$

c) Design of DC link capacitor (Cdc)

The choice of dc link capacitor depends upon the power flow between ac and dc power of Filter [8]. The design of C_{dc} can be expressed by computing the energy balance of SAF. The converter power (P_{con}) is given by [6],

$$P_{conv} = P_s(t) - P_L(t) = \overline{P}_{conv} + \tilde{P}_{conv} \tag{4}$$

where the direct and alternating components of P_{conv} and considering constant power loss.

The converter injects the harmonic current and fundamental reactive current, thus the expression of average value of P_{conv} is given by,

$$\overline{P}_{conv} = \frac{1}{2}V_s\left(\sum_2^{\infty} I_h + I_{rms1}\sin q_1\right) \tag{5}$$

where V_s, I_h and I_{rms1} are the rms value of supply voltage, harmonic current and the fundamental load current, $\sin q_1$ is the sine of the phase angle between the V_s and I_{rms1} and h is the harmonic order The energy stored in C_{dc} is expressed as,

$$\frac{1}{2}C_{dc}\Delta V^2 dc = \left(\frac{1}{2}V_s\left(\sum_2^{\infty} I_h + I_{m1}\sin q_1\right) - p_{loss}\right)\Delta t. \tag{6}$$

Hence, the value of dc bus capacitor is obtained from the ripple content of the dc bus voltage and the voltage ripple is given by,

$$C_{dc} = \frac{\left(V_s\left(\sum_{2}^{\infty} I_h + I_{m1}\sin q_1\right) - 2p_{loss}\right)}{\Delta V^2{}_{dc}}\Delta t \tag{7}$$

The ripple is reduced by increasing the size of capacitor and the measurement of harmonic current, fundamental current and phase angle is required for the selection of dc link capacitor.

d) Power rating of filter (S_{SAF})

Filter is designed to mitigate harmonics by considering Total Harmonic Distortion along with the load power. To reduce the fundamental reactive power, sine of the fundamental phase angle is required to design the rating of the power device. The rating of the SAF is a function of the load characteristics [8]. The power rating is given by,

$$S_{SAF} = \sqrt{\frac{\sin^2 q_1 + THD^2}{1+THD^2}}S_{load} \tag{8}$$

where THD is considered for maximum load current distortion. For harmonic compensation, the rating of the filter is given by,

$$S_{SAF} = \sqrt{\frac{THD^2}{1+THD^2}}S_{load} \tag{9}$$

4. OFF LINE MEASUREMENT OF ELECTRICAL PARAMETERS

The design parameters require information about harmonic current, fundamental current, phase angle, THD and apparent power. The magnitude of the fundamental component and phase angle is determined from the known value of instantaneous load voltage and current using Hilbert & Wavelet transform. Hilbert transform gives the complex form of signal and the decomposition of original signal (source voltage and current) and Hilbert transform signal using Wavelet transform extract the electrical variables required for filter design [9,10].

a) Conversion of signals using Hilbert transform

Hilbert transform is a linear operator that takes a function, f(t), transformed to H(f(t)) , with the same domain. It represents the analytical signal for the function f(t) which is extended to complex plane. The Hilbert transform is defined using the Cauchy principal value [11, 12].

$$hl(t) = H(f(t)) = -\frac{1}{\pi}p\int_{-\infty}^{\infty}\frac{f(\eta)}{\eta - t}d\eta$$

$$hl(t) = \frac{1}{\pi}p\int_{-\infty}^{\infty}\frac{f(\eta)}{t - \eta}d\eta \tag{10}$$

P is the Cauchy principal value of the integral, hl(t) is the Hilbert transform signal.

The distorted load current signal with a phase shift of $q_{1°}$ is given by,

$$i_{L1a}(t) = \sum_{h=1}^{\infty} I_{mah}\sin(h\omega t - q_h)$$

$$\omega = \frac{2\pi}{T} \tag{11}$$

where T is the time period and h is the harmonic order.

$$hl(t) = H(I_{L1a}(t)) = \sum_{h=1}^{\infty} I_{mah}\cos(h\omega t - q_h) \tag{12}$$

b) Extraction of electrical parameters using wavelet transform

Wavelet analysis is the process of transforming the waveforms defined in the time domain into a time-frequency domain using wavelet functions called mother wavelet. This process is achieved through calculating the wavelet coefficients at every scale (frequency) and position (time) thus obtaining the Continuous Wavelet Transform (CWT). This represents the continuous wavelet coefficients that signify how close the original waveform is to the wavelet function [13] at the particular scale and position. The wavelet functions at every scale and position are called daughter wavelets and the signal is represented by the following equation

$$f(y) = \sum_m s_j(m)\phi(t-m) + \sum_m\sum_{j=0}^{j-1} k_j(m)2^{j/2}\psi(2^j t - m) \tag{13}$$

Where Cj is the j level scaling coefficient, Dj is the j level wavelet coefficient, Φ(t) is the scaling function, Ψ(t) is wavelet function, j is the highest level of wavelet transform, t is the time.

In order to decrease the computational effort further while preserving the identification of the harmonic components required for the analysis, the Discrete Wavelet Transform (DWT) should be used. In DWT, the original waveform is decomposed into approximation and detailed coefficients at the first stage. Successive

decompositions are performed on the approximation coefficients only with no further decomposition for the detailed coefficients, hence obtaining the Multi-Resolution Analysis (MRA).

Daubechies wavelet is highly recommended for the decomposition to measure the power quality which is illustrated in Figure-2. The approximation and detailed coefficients at scale j are written as caj and cdj, to detect the harmonic content in distribution system.

The rms value of the quantity is measured [14-16] from the following equation

$$V_{rms}(or)I_{rms} = \sqrt{\frac{1}{m_j}\sum_k \left(cd_j(k)\right)^2} \tag{14}$$

where mj is the number of detailed coefficients at scale j.

The total harmonic distortion is calculated by,

$$THD = \sqrt{\left(\frac{I_{rms}}{I_{fund}}\right)^2 - 1} \tag{15}$$

where I fund is the fundamental component of the load current.

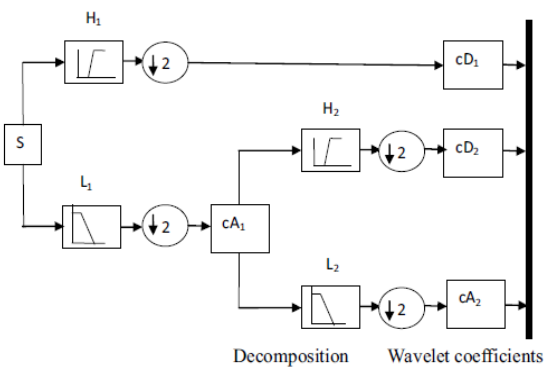

Figure-2. Schematic diagram representation of decomposition of wavelet coefficients.

The true rms value and fundamental component (Vfa or Ifa) of the signal is obtained from the Wavelet coefficients of the original signal (IL1a(t)) and Hilbert transformed signal (hl(t)). Table-1 shows the comparison of the calculations such as true rms value, fundamental rms value, phase angle and % THD obtained from the Wavelet Transform and Fast Fourier Transform. The results obtained are same in both the cases for different types of linear and nonlinear load connected in parallel to the supply mains, but the Wavelet Transform has less computational effort.

The procedure for the design of filter is depicted in Figure-3. The design of the SAF needs the measurement of the 1-phase supply voltage ($V_s(t)$) and current($I_L(t)$). The following variables and parameters are calculated to design the filter components (L_f ,C_{dc}).

- V_{rms},I_{rms}, V_{rmsf}, I_{rmsf}, q_1 and THD using Hilbert and Wavelet transform
- kVA rating of load and Shunt Active Filter
- Initial value of reference dc bus voltage($V_{dc,ref}$), per phase filter Inductance(L_f) and dc bus capacitance(C_{dc})
- Maximum value of the derivative of filter current

If the below equation is satisfied, then the size of the passive components (L_f, C_{dc}) and reference value of dc bus voltage is obtained.

$$V_{dc} \geq 2\left(\left(L_f \frac{di_f}{dt}\right)_{\max} + \hat{V}_s\right) \tag{16}$$

If the condition is not satisfied, the reference dc bus voltage, switching frequency, ripple content of filter current are increased by a factor Δ and the ripple content of dc bus voltage is decreased by a factor Δ. Once the condition is satisfied, the values of the filter components are obtained.

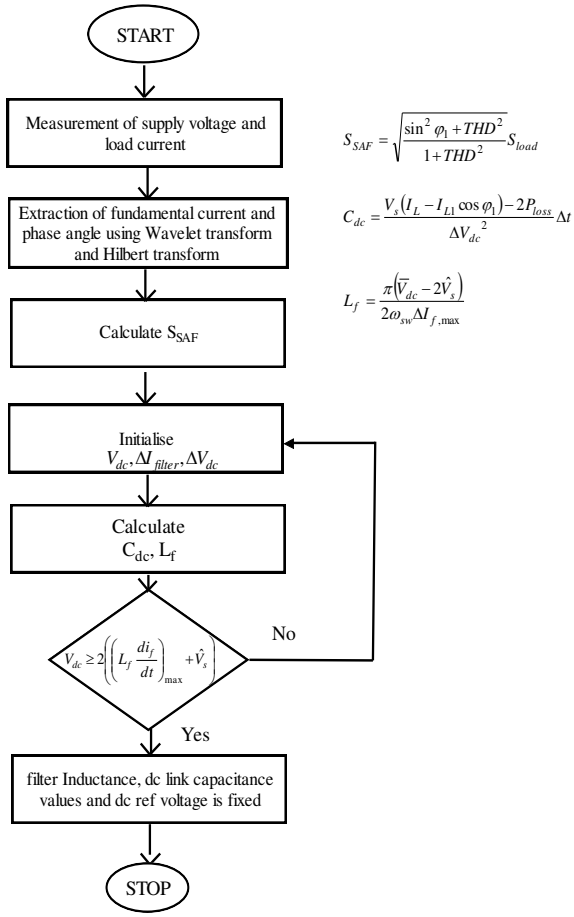

Figure-3. Flow chart for the shunt active filter design.

5. CONTROL ALGORITHM FOR REFERENCE CURRENT GENERATION

Power quality problems are tackled using different methods and the categorization of these methods is based on the closed loop control strategy and the selected reference current generation methods for Shunt Active Filter [17-21]. The reference current may be a fundamental component or harmonic component which decides the closed loop control strategy. In Direct Current Control (DCC) strategy, reference current is the harmonic current and in Indirect Current Control (IDCC), the reference current is the fundamental current. Due to less system complexity and ease of measurement of the supply current, IDCC [17] is preferred over DCC as the control strategy. In this chapter, the popularly used conventional control algorithm, Synchronous reference frame (SRF).

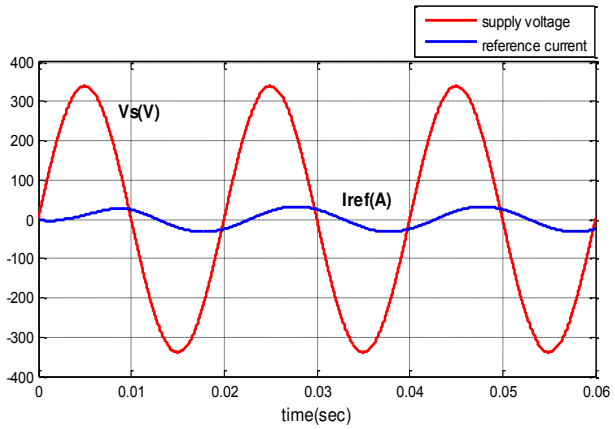

Figure-4. Supply voltage and reference current waveform of Induction motor load.

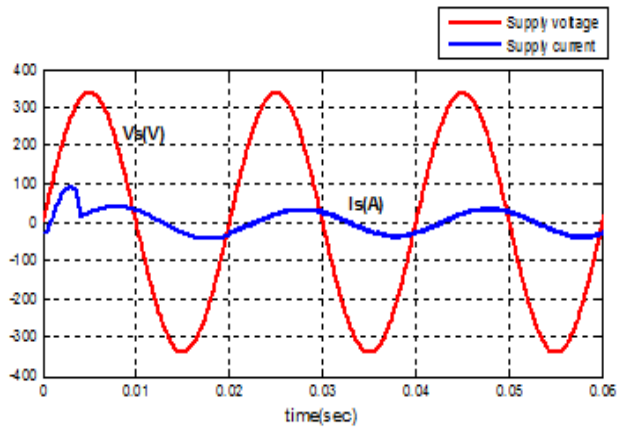

Figure-5. Supply voltage and current waveform of induction motor load.

For Induction motor load, the fundamental current generated by the SRF has the phase shift of 44° with respect to the supply voltage as discussed in section.2 is depicted in Figure-4. According to IDCC strategy, the supply current follow the reference current, so the supply current has the phase shift of 44° which is shown in Figure-5.

a) Drawbacks of SRF

a) It is not suitable for unbalanced load conditions
b) If the load current has the fundamental phase angle of q_1°, the reference current generated has the phase shift of same q_1°, which gives poor performance in fundamental reactive power compensation
c) There is an unnecessary complexity and high computational burden to control the system due to transformation (abc-dq-abc)
d) Filtering the dc component using Butterworth LPF gives poor dynamic response

6. MODIFIED CONTROL ALGORITHM

The 3-phase, star connected balanced supply voltage (abc sequence) and load currents are defined by,

$$V_{as} = V_{ma} \sin \omega t \tag{17}$$

$$V_{bs} = V_{mb} \sin(\omega t - 120°) \tag{18}$$

$$V_{cs} = V_{mc} \sin(\omega t - 240°) \tag{19}$$

$$I_{L1a} = \sum_{h=1}^{\infty} I_{mah} \sin(h\omega t - q_h) \tag{20}$$

$$I_{L1b} = \sum_{h=1}^{\infty} I_{mbh} \sin(h(\omega t - 120°) - q_h) \tag{21}$$

$$I_{L1c} = \sum_{h=1}^{\infty} I_{mch} \sin(h(\omega t - 240°) - q_h) \tag{22}$$

where h is the harmonic order and qh is the phase angle of corresponding harmonic order.

The load current contains the fundamental component and harmonic current components. The fundamental current component from load current is derived by the following equations.

The three phase load current is transformed to 2 - phase quantity by abc - dq transformation and is given as

$$\begin{bmatrix} i_{\alpha r}(t) \\ i_{\beta r}(t) \end{bmatrix} = \frac{2}{3} \begin{bmatrix} 1 & -\frac{1}{2} & -\frac{1}{2} \\ 0 & \frac{\sqrt{3}}{2} & -\frac{\sqrt{3}}{2} \end{bmatrix} \begin{bmatrix} i_{La}(t) \\ i_{Lb}(t) \\ i_{Lc}(t) \end{bmatrix} \tag{23}$$

$$\begin{bmatrix} i_{dr}(t) \\ i_{qr}(t) \end{bmatrix} = \begin{bmatrix} \sin\theta & -\cos\theta \\ \cos\theta & \sin\theta \end{bmatrix} \begin{bmatrix} i_{\alpha r}(t) \\ i_{\beta r}(t) \end{bmatrix} \tag{24}$$

where 'r' denotes the reference value

The variables idr(t) and iqr(t) represent the transformed currents in the dq frame which has high frequency ripples. The Moving Average Filter (MAF) is implemented to eliminate ripples of dq component of load current. This filter is a simple FIR filter used to average out the higher frequency components to zero while retaining the DC component. The average value of last N samples are given as [22],

$$y[k] = \frac{1}{N}\begin{bmatrix} x(k) + x(k-1) + x(k-2) ..... + \\ x(k-N+1) \end{bmatrix} \tag{25}$$

The Corresponding transfer function is,

$$H(z) = \frac{1}{N}\begin{pmatrix} 1 + z^{-1} + z^{-2} + ... + \\ z^{-N+1} \end{pmatrix} \tag{26}$$

$$H(z) = \frac{1}{N}\frac{1 - z^{-N}}{1 - z^{-1}} = \frac{1}{N}\left[\frac{1}{1 - z^{-1}} - \frac{z^{-N}}{1 - z^{-1}}\right] \tag{27}$$

$$H(z) = \frac{1}{N}\left[\frac{z}{z-1} - \frac{z}{z-1}z^{-N}\right] \tag{28}$$

The block diagram representation of the above equation is shown in Figure-6.

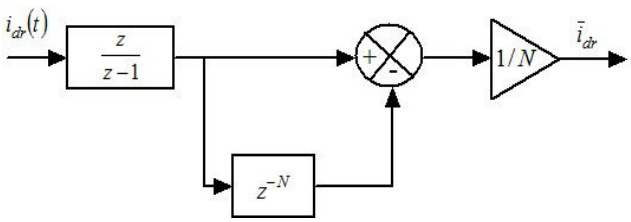

Figure-6. Averaging i_{dr}.

Similarly, the average value of the quadrature axis component is obtained from the above equations. The average value of dq frame for the measurement of fundamental current is acquired by taking half cycle of the supply frequency of the system because the load current is a balanced symmetrical wave.

Using equation. (24) to equation. (28), the average value of dq components of 3 - phase load current is obtained.

$$\bar{i}_{dr} = \frac{I_{m1}\cos q_1}{2} \tag{29}$$

$$\bar{i}_{qr} = \frac{I_{m1}\sin q_1}{2} \tag{30}$$

The maximum value of the fundamental current from the above equations is described by

$$I_{dqr} = 2\sqrt{\bar{i}_{dr}^{\,2} + \bar{i}_{qr}^{\,2}} = I_{m1} \tag{31}$$

The fundamental current obtained from the above value is given by,

$$\begin{bmatrix} i_{ra}(t) \\ i_{rb}(t) \\ i_{rc}(t) \end{bmatrix} = [I_{m1}]\begin{bmatrix} \sin\omega t \\ \sin(\omega t - 120°) \\ \sin(\omega t + 120°) \end{bmatrix} \tag{32}$$

The reference current is generated by adjusting the magnitude of the fundamental current with the voltage control loop gain. The voltage controller compares the actual dc bus voltage with reference voltage (Vdc, ref) and the error is given to the PI controller. The gain of the PI controller adjusts the fundamental and the reference current is given by [23-25],

$$i_{refa}(t) = \begin{bmatrix} i_{ra}(t) \times (1 + K_p(V_{dc,ref}(n) - \\ V_{dc}(n)) + K_i(V_{dc,ref}(n-1) \\ -V_{dc}(n-1)) \end{bmatrix} \tag{33}$$

Similarly reference current for other two phases are generated from the other phase current. Only the magnitude of the fundamental current is adjusted by PI controller, so equation (33) gives the reference current without any phase shift. The magnitude Im1 is equal to the fundamental component of load current.

Even though the load current has the phase shift with respect to the supply voltage, the above reference current expression gives the signals, containing the fundamental component without any phase shift.

Table-1. Calculation of fundamental load current and phase angle using FFT and DWT.

Load types	I_L(A)		I_{L1}(A)		$q_{1°}$		THD(%)	
	Wave	FFT	Wave	FFT	Wave	FFT	Wave	FFT

	let		let		let		let	
Rectifier load (21.3kW)	29.76	29.79	28.7	28.78	0.033	0.06	27.52	27.05
Electric drive (24.6kW)	34.23	34.89	18.3	18.44	3.34	3.3	158.5	157.0
Induction motor (17.1kW)	33.4	32.9	33.34	32.85	-44.45	-44.2	5.62	5.31
Rectifier and Induction motor (22.5kW)	40.85	40.75	39.67	39.57	-39.21	-39.5	24.51	24.56

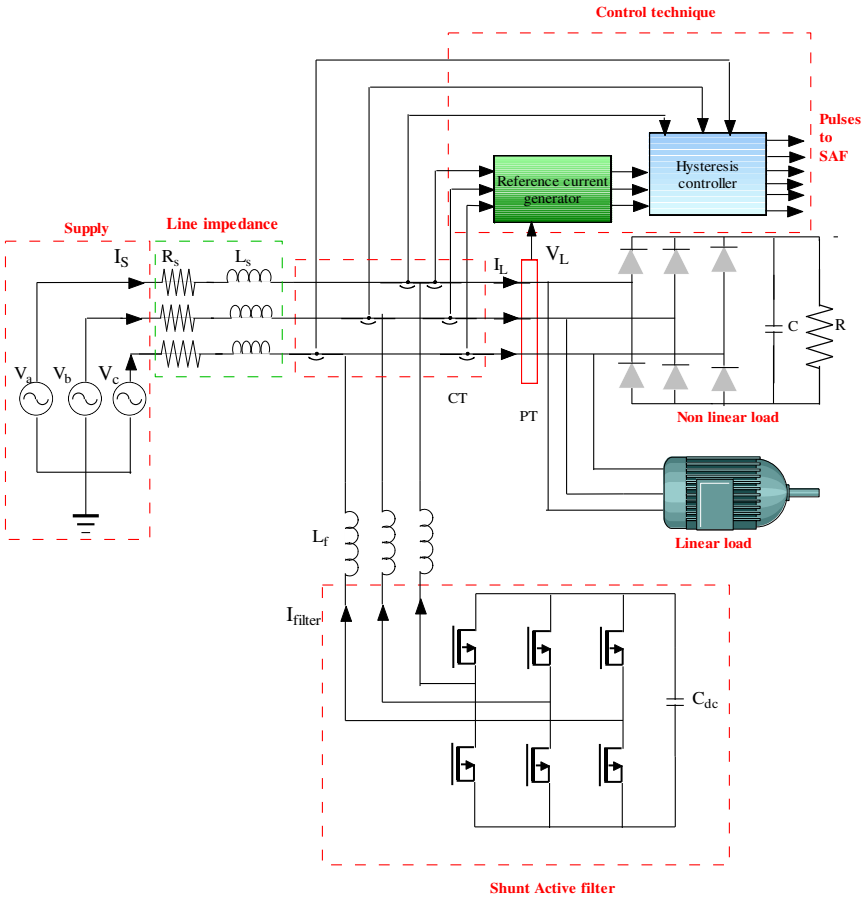

Figure-7. Circuit diagram of the three phase three wire system configuration.

7. CIRCUIT DIAGRAM OF THE SYSTEM CONFIGURATION

The system configuration considered for the testing is given in Figure-7. The three phase supply with source impedance is connected with three phase diode bridge rectifier and induction motor load. The supply voltage and current are measured and the variables required for the design of filters are procured. The values of the passive components and the rating of the filters are derived based on the flowchart. Even operation requires proper switching of the power devices of the Shunt Active Filter. These switching pulses are generated by the hysteresis current controller which compares actual supply/filter with the fundamental/harmonic current generated by the reference current generator.

a) Selection of hysteresis band for current controller

The Hysteresis controller maintains the supply/harmonic current and the reference within the hysteresis band. It is clear that the harmonic correction in supply mains depends upon the hysteresis band (hb), and the typical range of hb to keep the THD of the supply current within 5% as specified by IEEE 519 [5] is

$$h_b = G_h I_{m1}$$

Gh is the range from 0.0001 to 0.01.

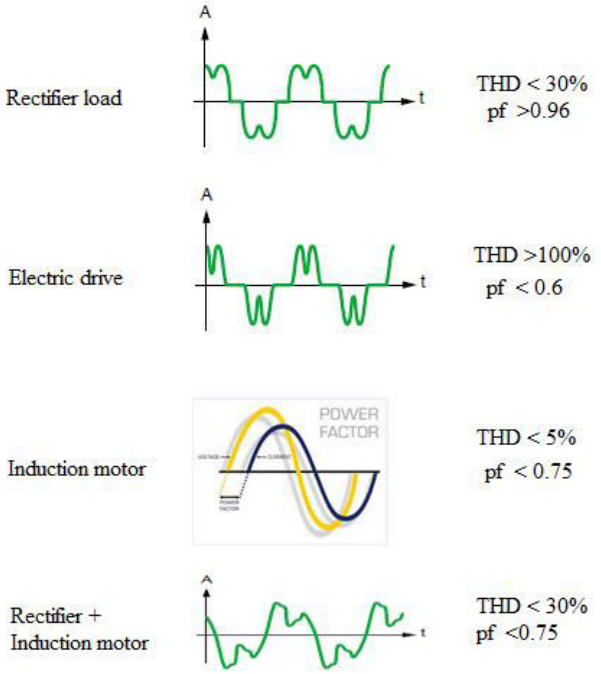

Figure-8. Current waveforms for different types of load with THD and power factor.

b) Types of load for testing

Power quality is analyzed in various buildings of SASTRA. Based on the results, the load is characterized by linear load, nonlinear load, highly nonlinear load and the combination of linear and nonlinear load. To Simulate the model in MATLAB Simulink, the three phase Induction motor is considered as a linear load, Rectifier with RC load is a non linear load, Rectifier with R and high value of C is taken as highly nonlinear load which resembles the electric drive characteristics and parallel connection of Induction motor and Rectifier load with the mains is considered as the combination of linear and nonlinear load. The design of filter is done for the maximum load condition. The different types of loads considered for design of the filter is depicted in Figure-8 and they are characterized by the THD and power factor

8. DESIGN PARAMETERS OF SHUNT ACTIVE FILTER

The three phase supply voltage of 415V, 50Hz with the line impedance of (0.86 + 0.01e-6) Ω is considered. The three phase diode bridge rectifier of 36 kVA with variable RC load and the linear load of 18 kW is connected to the supply mains. Out of many loads considered for calculating the characteristic parameters in Table-1, the worst case load is considered for design. Table-2 gives such type of loads (3-phase power) with their characteristic parameters (supply current, phase angle and THD) and the designed parameters. The maximum value of filter inductance, dc link capacitance and reference dc bus voltage is chosen in order to reduce the ripple content of filter current and dc bus voltage and the system parameters are given in Table-3.

9. SIMULATION CIRCUIT OF AVERAGE dq FRAME

The Average dq frame algorithm along with the system configuration is simulated using MATLAB Simulink. The power system block set is used to develop power electronics circuit and various types of load. The control algorithm and Hysteresis Current Controller are developed using Simulink blockset.

Table-2. Characteristics parameters.

Types of load	Calculated values using transforms					Designed parameters			
	I_L A	q_1 degree	THD %	S_{load} kVA	S_{SAF} kVA	L_{dc} µH	C_{dc} µF	f_{sw} kHz	$V_{dc,ref}$ V
Rectifier load (20.66kW)	29.76	0.033	27.52	21.39	5.68	564	240	18	800
Electric drives (13.25kW)	34.33	3.3	157	24.67	19.52	116	304	5	700
Induction motor (16.22W)	31.5	-44.21	5.62	22.64	15.75	386	3850	13	780
Rectifier + Induction motor (22.1kW)	40.85	-39.21	24.51	29.36	19.33	297	2860	11	760

Table-3. System parameters.

Parameter	Value
Supply voltage	240 V
R_s, L_s	0.86Ω, 0.01µH
Frequency	50 Hz
Switching frequency	11kHZ
Nonlinear load	30 kW
Linear load	18 kW
L_f	300 µH
C_{dc}	3000µF

VOL. 12, NO. 24, DECEMBER 2017 ISSN 1819-6608
ARPN Journal of Engineering and Applied Sciences

$V_{dc,ref}$	800V

Five different stages are involved in the implementation of the algorithm:

1. Transformation of load current from 3-phase to 2-Phase frame
2. Averaging the 2-phase quantities
3. DC bus voltage control
4. Reference current generation
5. Pulse generation using Hysteresis controller

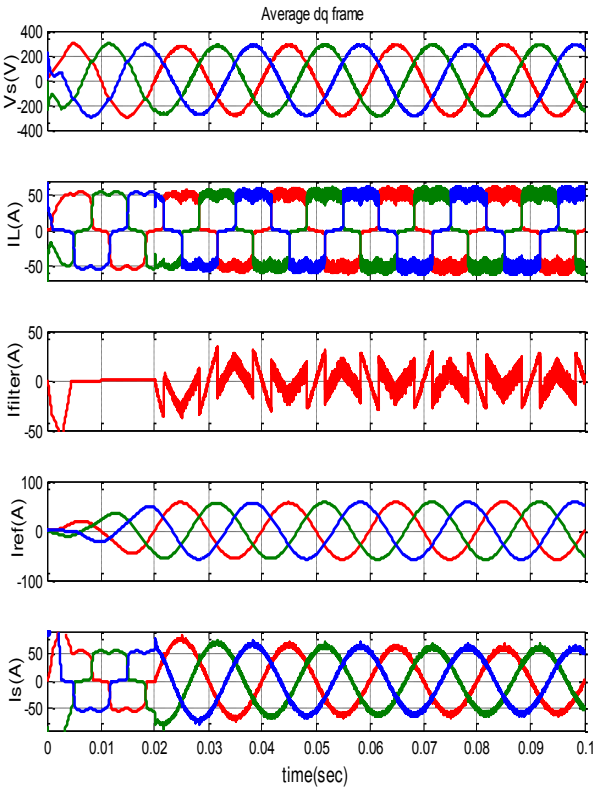

Figure-9. Simulation results of supply voltage, load current, filter current, reference current and supply current for rectifier load.

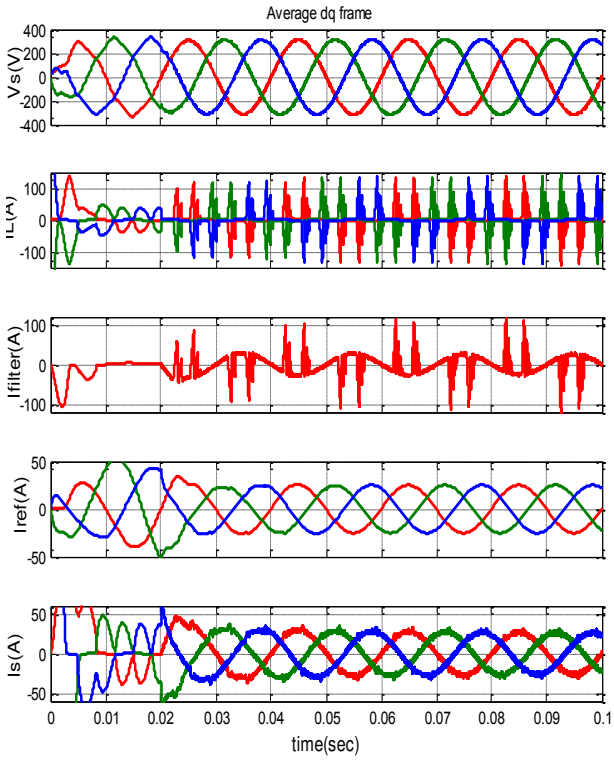

Figure-10. Simulation results of supply voltage, load current, filter current, reference current and supply current for electric drive load.

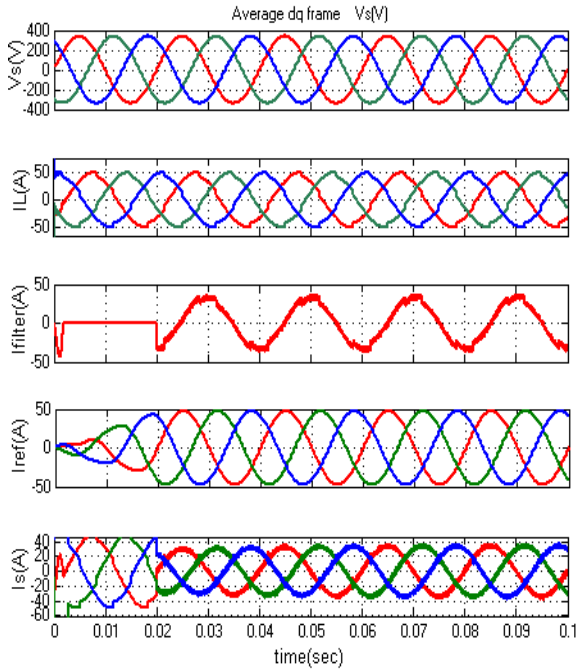

Figure-11. Simulation results for the supply voltage, load current, filter current, reference current and supply current for induction motor load.

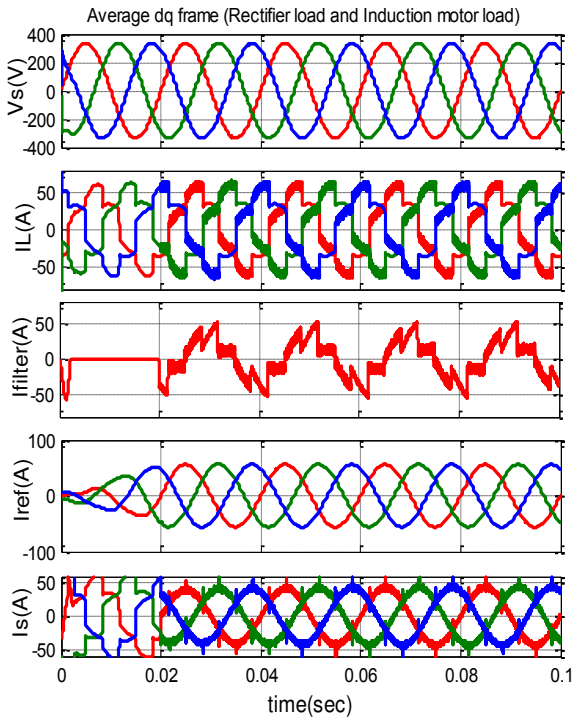

Figure-12. Simulation results for the supply voltage, load current, filter current and supply current for rectifier and induction motor load.

10. RESULTS AND DISCUSSIONS

The control algorithm is developed in MATLAB-Simulink and the waveforms are shown in Figure-9 - Figure-12. The results show that the control algorithm generated by the average dq frame generates fundamental current and the reference signal is generated from the voltage control loop. The reference current is compared with the supply current using hysteresis controller. The 4 different loads the supply current THD is reduced after compensation and the supply current is in phase with the supply voltage. The designed parameter is well suited for all types of load.

11. CONCLUSIONS

The design of filter involves the calculation of rms value of supply voltage and current, fundamental current and voltage, phase angle and THD using Hilbert and Wavelet transform. The calculated values are compared with FFT analysis and the results are similar to FFT but the wavelet transform is better than FFT in terms of less complexity. The design of passive components are based on switching frequency, ripple content of filter current and reference value of V_{dc} of the SAF. The power rating of the SAF depends upon the fundamental phase angle, THD level of load current and power rating of load. Finally the maximum values of filter inductance and dc link capacitance are obtained based on the proposed process flow to minimize the ripple content of I_f and V_{dc}. The design is carried out in MATLAB.

REFERENCES

[1] Mendalek, Nassar and Kamal Al-Haddad. 2000. Modeling and nonlinear control of shunt active power filter in the synchronous reference frame. Proceedings of 9th IEEE International Conference on Harmonics and Quality of Power. 1: 30-35.

[2] R. Sriranjani and S. Jayalalitha. 2012. Comparison of passive active and hybrid filter in front end system. International Journal of communication engineering application. 3(3): 503- 506.

[3] R. Sriranjani and S. Jayalalitha. 2012. Investigation the performance of various types of filter. World Appiled Science Journal. 17(5): 643-650.

[4] Munduate, Alejandro, Gabriel Garcera and Emilio Figures. 2006. Robust control of a shunt active power filter for the medium voltage range based on a three-level neutral point clamped converter. IEEE Annual Conference on Industrial Electronics. pp. 2162-2167.

[5] Shafiuzzaman K., Khadem, Malabika Basu., Michael F. Conlon. 2014. Harmonic power compensation capacity of shunt active power filter and its relationship with design parameters. IET Power Electronics. 7(2): 418-43.

[6] Ricardo L´ucio de Araujo Ribeiro, Christian Cesar de Azevedo, Raphaell Maciel de Sousa. 2012. A Robust Adaptive Control Strategy of Active Power Filters for Power-Factor Correction, Harmonic Compensation, and Balancing of Nonlinear Loads. IEEE Transactions on Power Electronics. 27(2): 718-730.

[7] Krim F. 2011. Parameters estimation of Shunt Active Filter for Power quality improvement. 5th IEEE International Conference on Power Engineering and Optimization. pp. 306-311.

[8] Chaoui, Abdelmadjid, Jean-Paul Gaubert, Fateh Krim, and Laurent Rambault. 2008. On the design of shunt active filter for improving power quality. IEEE International Symposium on Industrial Electronics. pp. 31-37.

[9] Phen Chiak See, Vin Cent Tai, Marta Molinas, Kjetil Uhlen, Olav Bjarte Fosso. 2012. Enhanced active

power filter control for nonlinear non-stationary reactive power compensation. pp. 1-8.

[10] Shukla, Satyavati, Shivakant Mishra, and Bawa Singh. 2012. Online EMD with Fourier Transform for active shunt filter operation under non sinusoidal supply conditions. IEEE International Conference on Power Electronics, Drives and Energy Systems. pp. 1-5.

[11] Saini, Manish Kumar and Komal Dhamija. 2013. Application of Hilbert-Huang Transform in the Field of Power Quality Events Analysis. Proceedings of International Conference on Advances in Signal Processing and Communication. pp. 118-124.

[12] S. Avdakovic and A. Bosovic. 2014. Continuous Wavelet and Hilbert-Huang Transforms Applied for Analysis of Active and Reactive Power Consumption. Metrology and Measurement Systems. 21(3).

[13] W. Morsi and M. El-Hawary. 2010. Time-frequency single-phase power components measurements for harmonics and inter-harmonics distortion based on Wavelet Packet transform; Part I: Mathematical formulation. Canadian Journal of Electrical and Computer Engineering. 35(1): 1-7.

[14] T. Jin and W. Gu. 2012. Research of Power System Harmonic Analysis Based on Wavelet Theory. AMR. 588-589: 626-631.

[15] Kumar, Sunil G., Siva DVSS Sarma. and Venkatesh C. 2011. Wavelet transform based harmonic analysis and real power measurement. IEEE International Conference on Power Electronics. pp. 1-6.

[16] Surya Santoso, Edward J. Powers, and W. Mack Grady. 1994. Electric power quality Disturbance Detection Using Wavelet Transform Analysis. Proceedings of the IEEE-SP International Symposium on Time-Frequency and Time-Scale Analysis. pp. 166-169.

[17] S. Jain, P. Agarwal and H. Gupta. 2004. A Control Algorithm for Compensation of Customer-Generated Harmonics and Reactive Power. IEEE Transactions on Power Delivery. 19(1): 357-366.

[18] S. Gautam, P. Yunqing, Y. Kafle, M. Kashif and S. Hasan. 2014. Evaluation of Fundamental d-q Synchronous Reference Frame harmonic Detection Method for Single Phase Shunt Active Power Filter. International Journal of Power Electronics and Drive Systems. 4(1).

[19] Seong-Chon Choi1, Sang-Hoon Song, Dong-Rak Kim, Min-Ho Sin and Chung-Yuen Won. 2014. Shunt active power filter with enhanced dynamic performance using novel control strategy. IET Power Electronics. 77(12): 3169-3181.

[20] L.B. Garcia Campanhol, A Sérgio, Oliveira da Silva., Alessandro Goedtel. 2014. Application of shunt active power filter for harmonic reduction and reactive power compensation in three phase four-wire systems. IET Power Electronics. 7(11): 2825-2836.

[21] S. K. Jain, P. Agarwal and H. O. Gupta. 2004. A control algorithm for compensation of customer-generated harmonics and reactive power. IEEE Transaction on Power Delivery. 19(1): 357- 366.

[22] Sebastian Gomez Jorge, Claudio A. Busada, Jorge Solsona. 2014. Reduced order generalised integrator-based current controller applied to shunt active power filters. IET Power Electronics. 7(5): 1083-1091.

[23] R. Sriranjani, M. Geetha and S. Jayalalitha. 2013. Harmonics and Reactive Power Compensation Using Shunt Hybrid Filter. Research Journal of Applied Sciences, Engineering and Technology. 5(1):123-128.

[24] R. Venkatesh, S. Dinesh Kumar, R. Sriranjani and S. Jayalalitha. 2014. Performance analysis of harmonic reduction by shunt active power filters using different control techniques. Journal of Theoretical and Applied Information Technology. 63(1): 226-232.

[25] R. Sriranjani and S. Jayalalitha. 2011. Improvement of the dc bus voltage of shunt active filter using controllers. International conference on recent advancements in Electrical. Electronics and control, Engineering (ICONRAEeCE'2011). 187-191.